Supplementary Information: Trapping and manipulation of bubbles with holographic optical tweezers

I. EXPERIMENTAL SETUP

In this section, we will explain all the components of the two optical paths, trapping and imaging, that form the holographic optical tweezers set up. The laser used is a low coherence laser (coherent length of $\sim$ cm) but with consistent power stability $\leq$0.2% RMS(Opus 532, Laser Quantum).Absorption of light at the wavelength used is low enough to avoid heating, and thus possible thermophoresis or a gradient of the surface tension on the liquid-gas interface that may lead to maragoni flow, as in Sci.Rep 6, 34787 (2016). A $\lambda/2$ wave plate(WPMH05M-532, Thorlabs) is placed after the laser for a fine tuning of polarization state as the spatial light modulator LETO, Holoeye requires a horizontal polarization to perform phase only modulation. Two lenses (L1 and L2) with a focal distance of 35 mm and 150 mm are used to expand the laser beam in order to fill the active part of the spatial light modulator. Two mirrors (M) are placed to redirect the laser and ensure a small incident angle on the spatial light modulator. After reflection on the spatial light modulator, a 4f telescope (Fourier filter), formed by two lenses (L3 and L4) of focal distances of 100 mm and 150 mm, where the SLM plane is imaged on the exit pupil of the microscope objective(MO, Plan APO VC 100x/1.4, Nikon), is placed to meet two particular requirements: prevent vignetting of high frequency Fourier components and to slightly overfill the back aperture of the microscope objective as in a common optical tweezers set-up, as indicated in reference 18. If no hologram is displayed on the SLM, the optical setup can be used as a single beam optical tweezer. A dichroic mirror (DM) DMPL605 by Thorlabs is placed after the second lens of the 4f telescope and then most of the trapping light is redirected to the microscope objective. Illumination light is focused on the sample by a lens (L5), and optical contrast on the sample (S) is controlled by two iris diaphragms (ID). A micrometer three axis stage (St), NanoMax Stage (MAX311D, Thorlabs) with Differential Drives in an Open-Loop Piezos (TPZ001 and TSG001 by Thorlabs) configuration is used to manipulate the sample. Light scattered by the sample is then collected by the microscope objective and amplified 100X. The position of the dichroic mirror reflects wavelengths shorter than 605 nm and

thus the image is formed with the red part of the Tungsten-Halogen lamp spectra (QTH10, Thorlabs). The scattering of trapping light on the trapped particle, although small because of the 99% effective reflectance of the dichroic mirror, is enough to saturate the camera and thus an additional long pass filter (LPF) FELO600 by Thorlabs is placed before the camera (C, PL-B776F, Pixelink). Removing the filter with a low laser power permits observation of the holographic array on the sample, as shown in the insets of Fig.1 of the main manuscript. Although not clear on the schematic experimental set-up, Fig.1 of the main manuscript, first part of the optical set up, all trapping parts before the dichroic mirror, is placed horizontally on an optical table with active vibration isolation supports and the dichroic mirror reflects the laser upwards. Thus, most illumination part, from the lamp up to the mirror after the dichroic mirror, is placed vertically on an optical breadboard. This ensures a horizontal positioning of the sample, important to avoid the bubbles motion because of their flotation force. The rest of the imaging part (mirror, final lens and long pass filter) is again horizontal on the optical table.

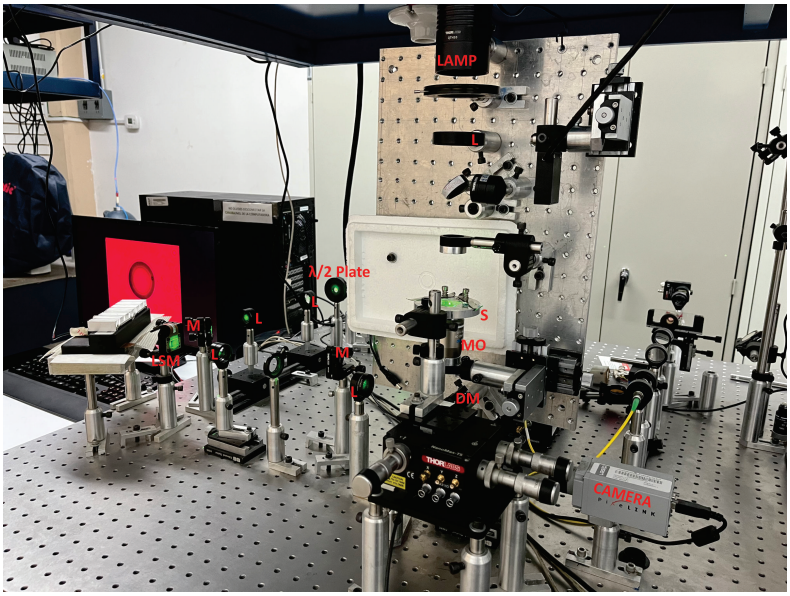

Figure 1: Photograph of the experimental set-up of holographic optical tweezers.

Finally, holograms are generated prior to the experiment with different holographic array diameters D_H using the Adaptive-Additive Algorithm from Review of Scientific Instruments 72, 1810 (2001). Hologram-to-actual size transformation is needed a priori and determined from the averaged distance between two trapped colloidal particles in two high intensity spots at different distances, giving a 10.2 pixels/μm transformation for a 800x800 pixels

hologram. Apart of the implementation of the 4f Fourier filter, additional configuration of the spatial light modulator, namely the range of applied voltages on the pixels, is useful to reduce the intensity of the zero-order diffraction, a high intensity beam located in the center of the holographic array that reduces the efficiency of the bubble trapping. Figure 1 shows an actual image of the experimental set-up. The number of points forming the array was defined as a good balance between trapping strength and avoiding repulsion from the array as two bubbles are brought to contact.

II. SAMPLE PREPARATION

Figure 2 shows photographs of the foam inside the syringe system at different cycle number, exhibiting tonality ranging from colorless clear when the preparation begins, to white when it is properly formed. Turbidity is caused by light scattering by the bubbles and it is a clear indication of the formation of a colloidal suspension. Due to the presence of the low diffusion gas, the foam seems to be stable to the naked eye for several hours even when the foam is taken out of the syringe system.

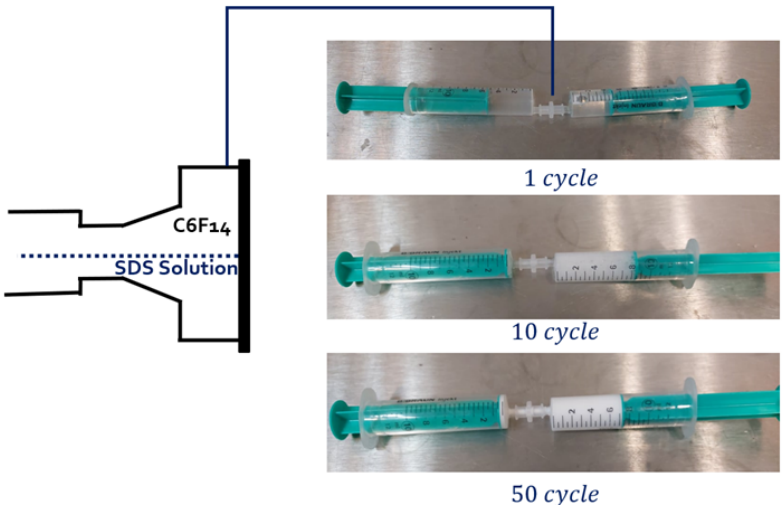

Figure 2: Foam appearance at different cycles in its preparation process.

Figure 3(a) shows an image of the prepared foam visualized by bright field microscopy using a Nikon Eclipse Ti microscope and a 10X microscope objective, and figure 3(c) presents the corresponding percentage distribution of bubble sizes just after loading the sample. Figure 3(b) and (d) presents the same information as above but after 60 minutes. A similar

distribution was found, with minimal differences in the mean size and standard deviation that can be attributed to changes in the lower and upper limits of the binarization used to determine the distribution. All size measurements were made in ImageJ. Distribution is centered at 34.06μm with a deviation of 5.32μm at 0 minutes, and 32.93μm with a deviation of 5.07μm at 60 minutes. The foam seems to be stable as the distribution does not change significantly within a 4 hr window observation, indicating that the gas diffuses slowly to the solvent. This feature was also observed when two bubbles are in contact, despite a coalescence process is expected, finding that the size of the two bubbles remains constant within the experimental time window required to perform adhesion force measurements. Thus our experiments lies within the regime where the foam is stable.

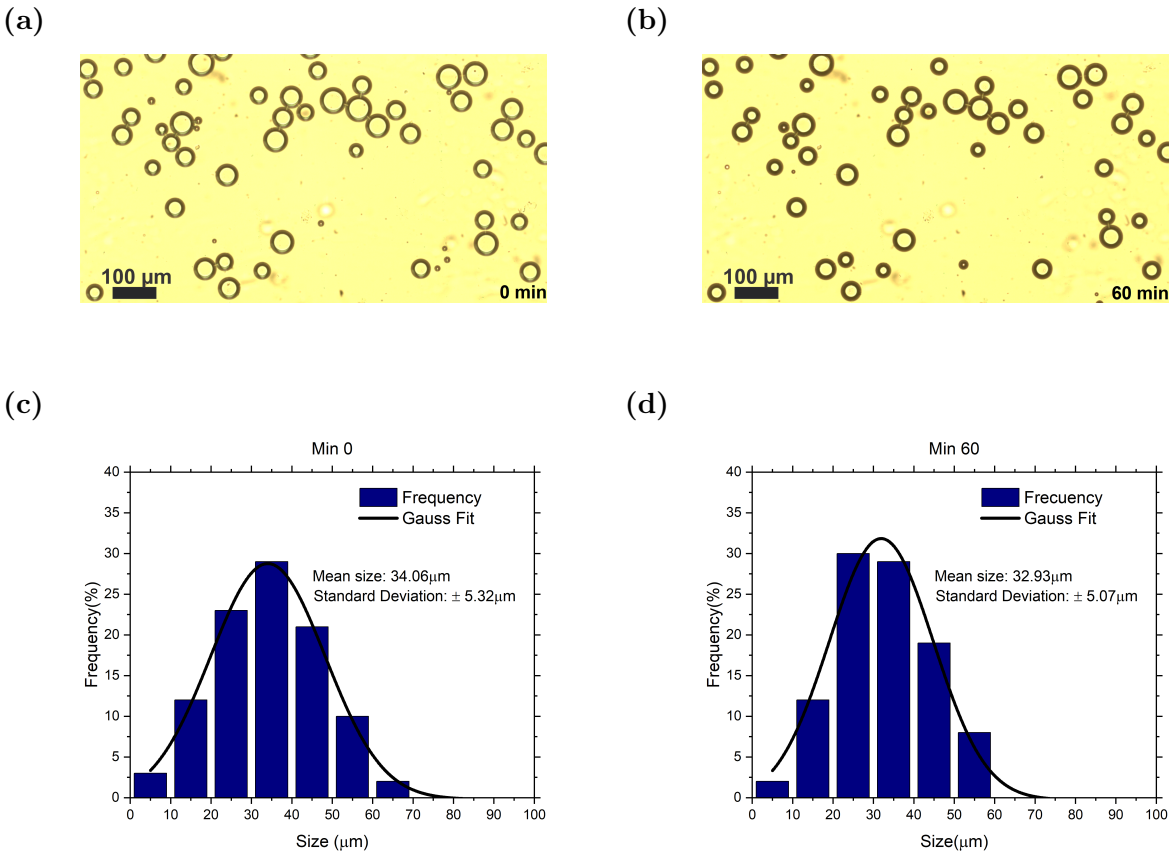

Figure 3: (a) and (b), bright field microscopy images for foams at 0 and 60 min after preparation. (c) and (d), size histograms determined from (a) and (b).

III. RAY TRACING APPROXIMATION FOR THE ESTIMATION OF THE TRAPPING FORCE

Several theoretical approaches for the determination of the trapping force on optical tweezers are available in the literature (see main manuscript for corresponding references). Range validity depends mainly on the relation between the wavelength of the trapping laser and the size of the trapped object. As in this case the bubble size is bigger than the trapping wavelength, the ray tracing methodology is valid and used to estimate the force map. In this section we will follow a procedure outlined before, reference 21 in the manuscript, for the calculation of the trapping force using the ray tracing approximation. The first requirement is the calculation of the refracted angle for a ray initially traveling parallel to the optical axis at a distance x from the center of the bubble. The trapping force should be proportional to the refracted angle, being a quantification of the change of momentum of the incident photon. Thus the force is computed as:

$$F(y_0) \propto \int_{-r}^{r} I(y + y_0)\Delta(y)dx$$

where $I(y)$ is the intensity profile, r is the radius of the bubble, and y_0 is the distance between the center of the intensity profile and the center of the bubble, $\Delta(y)$ is the trapping contribution by a single light incident at distance y from the center of the bubble:

$$\Delta(y) = \frac{y}{r}\sqrt{1 - \left(\frac{y}{nr}\right)^2} - \frac{y}{nr}\sqrt{1 - \left(\frac{y}{r}\right)^2}$$

and $n = n_{air}/n_{bubble}$ is the index of refraction ratio.

A simple 1D calculation is performed by considering two Gaussian spots with variance equals to 10% the diameter of the control bubble, and separated a distance of 2 arbitrary units. This value was selected to fit experimental results at a given D_H/D ratio and laser power, but it was kept constant for other experimental conditions, and thus it is not considered to be a free parameter. For the calculation of the trapping force at different laser powers, the bubble size was selected to match the center-to-center distance between spots, as shown schematically in Fig.4b of the main manuscript and intensity profiles at different laser powers were modified accordingly. Optical trapping calculation when the bubble size changes due to diffusion of gas to the solvent is performed, keeping fixed the distance between the Gaussian spots and reducing the bubble size as shown in Fig.5b of the main manuscript.

An interesting feature was found for the case where the hologram size is smaller than the size of the bubble, as the ray tracing calculation is unable to reproduce the size of the zero force region found experimentally with the nominal D_H and D values. Instead, a region with a size of 0.9 $(D_H - D)$ was found. What we do with the experimental data gathered is overlap the fitting predicted by the algorithm, and then determine the point where the line crosses the y-axis at 0 at both left and right extremes. Subtracting those quantities is how we quantify the value where the region does not feel the trapping force. Then by plotting the experimental region where f=0 vs the simulation and fitting its linear behavior, a slope of 0.90±0.04 is obtained (See Figure 4). The origin of such difference may be attributed to the arbitrarily but fixed value of the Gaussian spot variance used. It is important to note that this feature is not affecting the estimation of the forces exerted on the bubbles using the tray tracing algorithm.

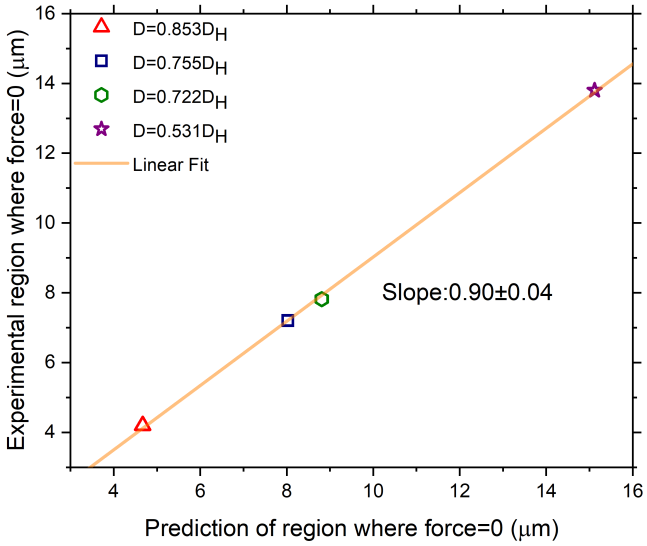

Figure 4: Comparative plot of the experimental vs estimated region where the force=0 and the bubble does not feel trapping.

Figure 5 shows the same information as in Fig.5 of the main manuscript but in a wider range of calculations, reduced for clarity reasons. The full range of calculations provides additional information at large Δy, where two force barriers are found, *i.e.* a region of negative force at negative values of Δy and the opposite at $\Delta y > 0$. Work must be done on the system to be able to overcome such barriers.

An example of the implementation of the above mentioned code, written in Mathematica,

is supplied as a supplementary material.

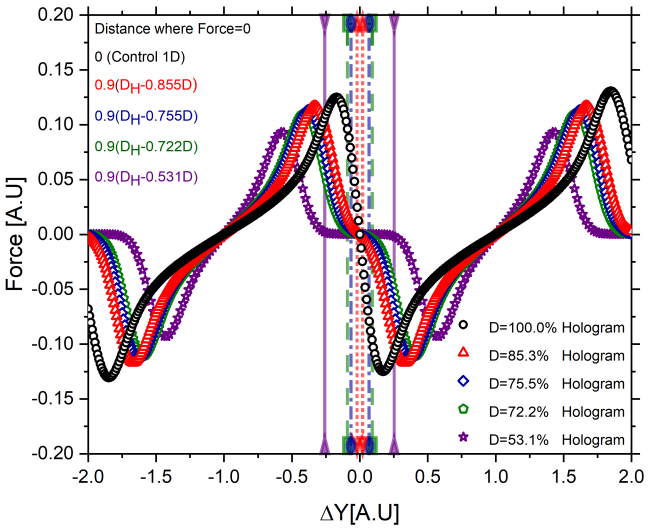

Figure 5: Ray tracing approximation for the case of various bubble sizes smaller than the hologram diameter, showing the repulsive region not shown for clarity on the main manuscript.

IV. ADHESION FORCE MEASUREMENTS UNCERTAINTLY

Since the laser power supply step increment is really small (2mW), obtaining the offset ΔY becomes the main source of error when calculating adhesion forces, the difficulty resides in determining the key moment of exact separation between the bubbles. A good criteria was found by converting the video to frames and applying a gray scale mask then use the software ImageJ to sharpen edges and fill holes of the bubbles so coordinates of their centroids could be measured and compared to the constant position of the laser holographic trap in order to obtain ΔY. Then it was observed when the bubble touch, the connection channel between them is also visible after the image manipulation explained but with the characteristic that the inside of the circumference of the trapped bubble D_1 is not fully filled, and when they separate the circumference of each bubble returns and the inside of D_1 is now fully filled (See Figure 6). The first frame when the circumferences become whole again and D_1 becomes filled, is the one used as a reference to measure the offset and compute the adhesion force. The separation point usually varies$\pm$5 frames, all of positions on that range are used to compute such force and an average is obtained with their corresponding uncertainty.

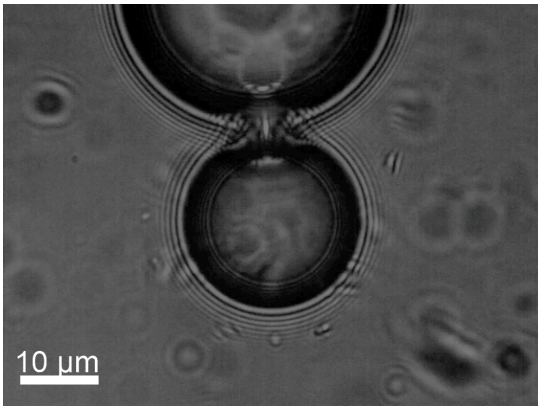

(a)

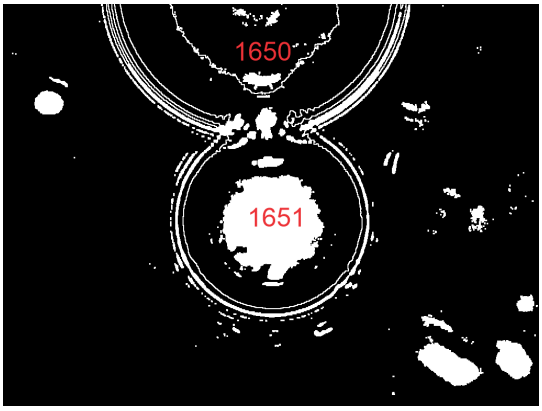

(b)

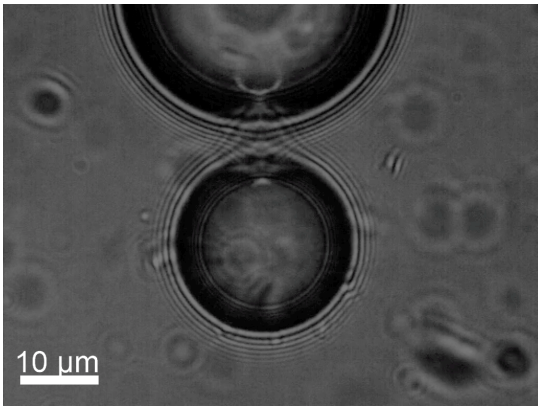

(c)

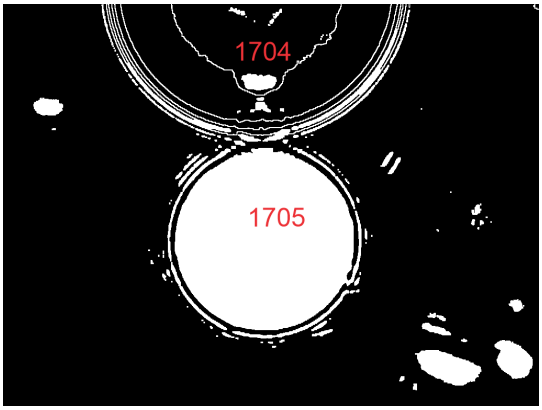

(d)

Figure 6: Graphical representation of the criteria to determine separation point between bubbles : (a) Frame with bubbles in contact, (b) Mask frame with bubble in contact (D_1 partially filled), (c) Fist frame with separated bubbles, (d) Mask frame of separation (D_1 totally filled). Numbers in (b) and (d) represent the particle etiquete assigned by ImageJ at the moment of analyzing.